Precise location of San Andreas Fault tremors near Cholame, California using seismometer clusters: Slip on the deep extension of the fault?

David R. Shelly,[1] William L. Ellsworth,[1] Trond Ryberg,[2] Christian Haberland,[2] Gary S. Fuis,[1] Janice Murphy,[1] Robert M. Nadeau,[3] and Roland Bürgmann[3]

Received 17 October 2008; revised 26 November 2008; accepted 2 December 2008; published 6 January 2009.

[1] We examine a 24-hour period of active San Andreas Fault (SAF) tremor and show that this tremor is largely composed of repeated similar events. Utilizing this similarity, we locate the subset of the tremor with waveforms similar to an identified low frequency earthquake (LFE) "master template," located using P and S wave arrivals to be ~26 km deep. To compensate for low signal-to-noise, we estimate event-pair differential times at "clusters" of nearby stations rather than at single stations. We find that the locations form a near-linear structure in map view, striking parallel to the SAF and near the surface trace. Therefore, we suggest that at least a portion of the tremor occurs on the deep extension of the fault, likely reflecting shear slip, similar to subduction zone tremor. If so, the SAF may extend to the base of the crust, ~10 km below the deepest regular earthquakes on the fault. **Citation:** Shelly, D. R., W. L. Ellsworth, T. Ryberg, C. Haberland, G. S. Fuis, J. Murphy, R. M. Nadeau, and R. Bürgmann (2009), Precise location of San Andreas Fault tremors near Cholame, California using seismometer clusters: Slip on the deep extension of the fault?, *Geophys. Res. Lett.*, *36*, L01303, doi:10.1029/2008GL036367.

1. Introduction

[2] Non-volcanic tremor was first recognized in the Nankai subduction zone in southwest Japan [*Obara*, 2002] and Cascadia [*Rogers and Dragert*, 2003], where its activity is correlated with slow slip events modeled to occur on the plate interface downdip of the megathrust zone [*Rogers and Dragert*, 2003; *Obara et al.*, 2004]. Since then, similar signals have been reported in several other subduction zones as well as beneath a few strike-slip faults. *Nadeau and Dolenc* [2005] identified tremor emanating from beneath the strike-slip San Andreas Fault (SAF) in central California near Cholame, and tremor triggered by passing surface waves from the 2002 M 7.9 Denali earthquake has been observed beneath several strike-slip faults in California [*Gomberg et al.*, 2008]. Tremor has also been reported beneath the rupture zone of the strike-slip Western Tottori earthquake in western Japan [*Ohmi et al.*, 2004]. Unlike Cascadia and southwest Japan subduction tremor, no geodetic deformation signal has yet been associated with tremor in these strike-slip environments [*Johnston et al.*, 2006].

[3] A major obstacle to understanding the mechanism of tremor has been the difficulty of accurately locating tremor hypocenters. Examining activity in western Shikoku, Japan, *Shelly et al.* [2006] located low-frequency earthquakes (LFEs), using body wave arrivals from these relatively impulsive portions of tremor. They concluded that the LFEs locate on the plate interface, downdip of the main seismogenic zone and coincident with the geodetically estimated region of slow slip. Using stacked records of LFEs, *Ide et al.* [2007] calculated a composite moment tensor solution for these events, with the result supporting the conclusion that they are generated by shear slip in the plate convergence direction. In an attempt to examine tremor outside the times of identified LFEs, *Shelly et al.* [2007a] employed a matched filter approach utilizing cataloged LFEs as waveform templates. They demonstrated that tremor could be explained as a sequence of many LFEs occurring in succession and used this technique to demonstrate migration of tremor in the updip and downdip directions at rates of 25–150 km/hr [*Shelly et al.*, 2007b]. Transferring this technique to tremor beneath the SAF presents a significant challenge however, because the basic building blocks of this approach, locatable LFEs, have not yet been identified here, although relatively impulsive events in the tremor have been seen at some stations [*Cannata et al.*, 2007].

[4] The premise of the template LFE approach is that tremor repeatedly exhibits a pattern of similar waveforms. In Japan, it was possible to locate portions of tremor by matching them with a similar, pre-located template event. In theory, however, it should be possible to estimate the differential locations of a similar event and the template used to detect it, provided the waveform similarity is high enough. This approach could provide precise relative locations for events close to the template, even if the absolute location of the template is not precisely known. In practice, however, small amplitudes and interfering sources reduce waveform similarity to the point where it is usually impossible to measure differential arrival times unambiguously via cross-correlation at a single station.

[5] During the fall of 2007, temporary arrays were installed near the Cholame tremor source. Three temporary arrays, each consisting of 10 3-component short period seismometers, were used in this study and are shown in Figure 1a. The permanent, borehole High Resolution Seismic Network (HRSN) was used as a fourth array, while Plate Boundary Observatory (PBO) borehole stations sup-

[1]U.S. Geological Survey, Menlo Park, California, USA.
[2]GeoForschungsZentrum Potsdam, Potsdam, Germany.
[3]Berkeley Seismological Laboratory, University of California, Berkeley, California, USA.

0094-8276/09/2008GL036367$05.00

plemented nearby arrays when sufficiently close (Figure 1a). In this paper, we demonstrate a method to use multiple nearby stations to dramatically increase the ability to resolve differential times in very noisy data. This allows us to obtain precise locations of similar events within the tremor.

2. Data and Method

[6] We examine tremor in the Cholame area for October 6, 2007 (UTC), a very active day (Figure 2a). Although tremor often lacks distinct phase arrivals, we identify one event within this tremor for which P and/or S-wave arrival times can be determined on some stations (Figure S1 of the auxiliary material).[1] We locate this event using a grid search technique, and find the best-fitting location to be 35.74° N latitude, 120.28° W longitude, and 26 km depth (Figure S2), which is almost directly beneath the surface trace of the SAF. While this event appears similar to a regular earthquake, its depth and waveform similarity to many other times of tremor confirms that it is an LFE, like those observed as part of tremor in SW Japan. We locate this event using a 1-D velocity model, approximating the model of *Thurber et al.* [2006] in this area. We then use this event as a "master event" and locate other events relative to it.

[7] We bandpass filter the data between 2 and 8 Hz to accentuate the tremor signal relative to the background noise. We use the waveforms of our identified LFE as an initial template selecting 6-seconds of data beginning shortly before the S-wave arrival at each station and use it to perform a systematic matched-filter search through the continuous data at intervals of 0.02 s, similar to the approach employed by *Shelly et al.* [2007a, 2007b]. We then sum the correlation coefficients across stations. An important component of this process is choosing appropriate correlation sum thresholds. Although the event detection problem allows for less stringent thresholds [*Shelly et al.*, 2007a], the event location problem is much more difficult because in addition to identifying similarity in the event, we must reliably measure differential times relative to the template. Low correlations normally make this impossible on a single station.

[8] To address this issue, we take advantage of the fact that for event pairs recorded at nearby stations the differential times should be nearly identical even if the station spacing is such that the absolute travel times vary significantly. This allows us to establish 4 sets of stations as "clusters", as shown in Figure 1a. We can then calculate a single differential time between a template and a detected

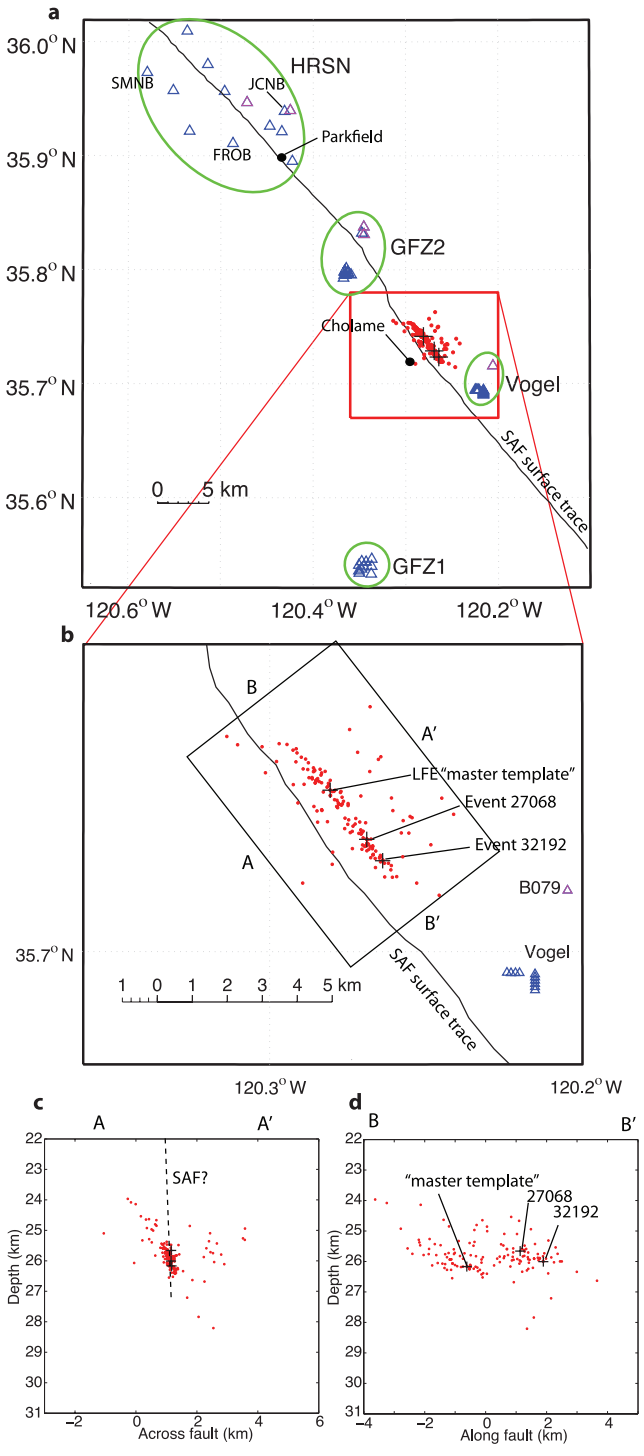

Figure 1. (a) Map of study region, including stations utilized in this study (triangles). Purple triangles are PBO borehole stations. Green ellipses indicate the four "clusters" of stations used together to calculate differential times. Although the HRSN is spatially extensive, it subtends a small angle from the tremor source. Red dots show locations of 148 correlated Cholame tremors on Oct. 6, 2007. Well-located tremors (those retaining more than 45 observations after relocation) from a combination of 5 templates are plotted. Red box outlines the region shown in Figure 1b. "SAF" is the San Andreas Fault. (b) Zoomed map view of tremor locations from part Figure 1a. Black crosses show the LFE "master template" as well as template (32192) and detected event (27068) from the example in Figure 3. (c) Across fault cross-section A–A′. Zero on the horizontal axis indicates the location of the SAF surface trace. (d) Along-fault cross-section B–B′. Note that these locations represent only those events well correlated with our master template on one day of activity.

[1] Auxiliary materials are available in the HTML. doi:10.1029/2008GL036367.

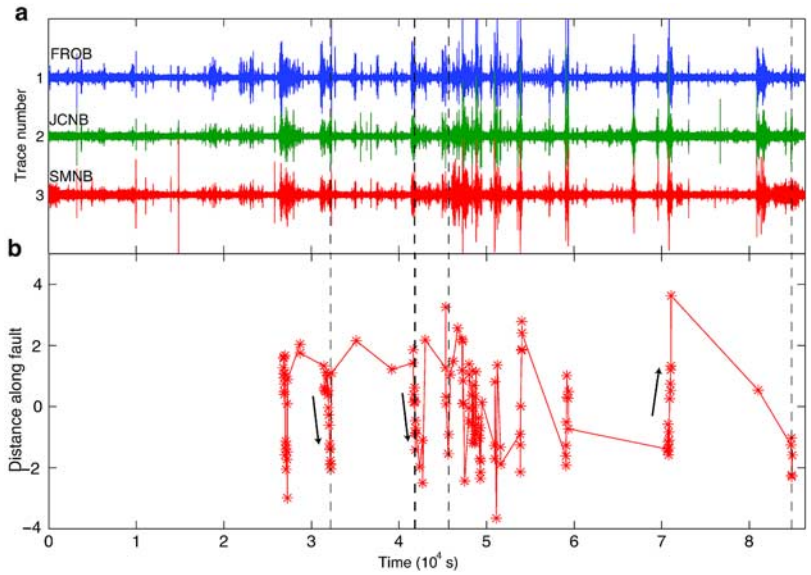

Figure 2. (a) Horizontal component waveforms from 3 HRSN stations for 24 hours beginning at 0:00:00 UTC October 6, 2007. Tremor is visible during much of this day, seen as the amplitude variations common to all stations. Dashed lines indicate the times of templates used for the locations shown in Figures 2b and 1b–1d. Two templates from nearby times are selected near a time of 4.2e4 seconds. (b) Tremor locations for events correlated with the templates, shown in the along fault direction versus time for the same period as Figure 2a. The northwest direction is positive. A few clear episodes of tremor migration can be seen on this small scale, marked by the black arrows. Migration on this small scale occurs at rates of 15–40 km/hr.

event using the timing of the peak of the correlation sum for each cluster. Although this technique gives only 4 differential times per event pair (one at each cluster), it provides a much more robust measurement than could be obtained at single stations. Figure 3 demonstrates the estimation of differential times between a template and a detected event. In this example, it is clear that the detected event lies to the

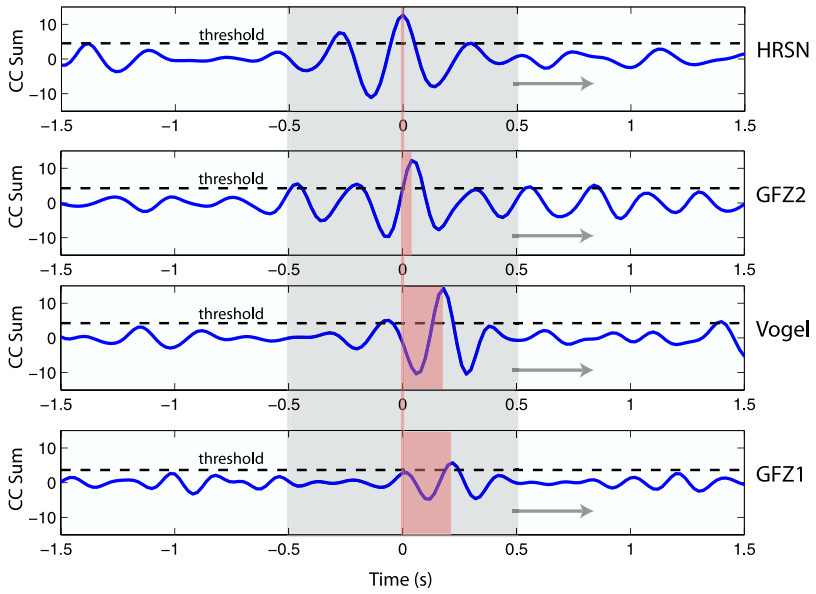

Figure 3. Cross-correlation (CC) sum functions (blue lines) for each seismometer cluster (template 32192, detected event 27068) demonstrating differential time estimation. Clusters are labeled at right (see Figure 1a) and ordered from north to south. The misalignment of peaks in the cluster correlation functions indicates that the source location of the detected event is spatially offset from the template. Delays at each cluster (relative to template and HRSN cluster) used for relative location are indicated by the width of the red shaded regions. Delays at southerly clusters GFZ1 and Vogel indicate that the detected event (ID #27068) is located north of the template (ID # 32192). Locations for these two events are highlighted in Figure 1. The gray shaded region shows the width of allowed 1-second window between peaks at different clusters.

north of the template event, since the delays are largest at the more southerly clusters.

[9] After summing correlation coefficients across stations within a cluster, we then sum all four clusters of stations. At this step, we record the time shifts that maximize the correlation sum at each time for each event pair. We allow for a time-shift of up to one second between different clusters, to accommodate small differences in hypocentral location between the template and detected event. Smaller limits strongly restrict the spatial extent of detected events, while a larger window increases the likelihood of cycle slip errors (misassociation of correlation peaks between clusters) in our differential time estimation. Based on the station geometry and S-wave velocity in this area, we expect a 1-second window to allow an epicentral range of approximately 4 km. We apply thresholds based on the median absolute deviation (MAD) of the correlation sum function to select events with waveform similarity high enough to allow successful location. See the auxiliary material for a discussion of the MAD as a detection threshold. To obtain accurate differential times, we require a correlation sum of at least 7*MAD at each cluster, and to assure that an event is strongly detected overall, we mandate an overall correlation sum value of at least 15*MAD above the median of the distribution. At most, we locate one event every 4 seconds. As a final step, we use the double-difference algorithm [*Waldhauser and Ellsworth*, 2000] to estimate the relative locations of events meeting these criteria from the arrival time differences. This algorithm is well suited to this problem since it directly utilizes our recorded time shifts as cross-correlation-based S-wave differential times.

[10] Besides our located LFE, we test a number of different templates identified through recursive selection whereby detected events from one template become new templates. To avoid possible artifacts from using a single starting location, we randomize initial locations of the detected events in three dimensions over a range of several kilometers surrounding the master template location. Adjusting the initial absolute locations by up to several kilometers changes the final absolute locations but has little effect on the relative locations.

[11] Any method to locate tremor locates the source of only a portion of the tremor waveform or obtains some average over many parts of the waveform. The method employed here allows location on a short timescale with potentially high precision, but is limited in that it only locates events within a few kilometers of our template that have similar waveforms.

3. Tremor Locations and Discussion

[12] Locations extend to the NW and SE of the master LFE, striking NW–SE, with epicenters following the trend of the SAF (Figure 1). Locations performed using randomized differential times in the same range as the real data show no such structure, suggesting that this feature is not an artifact of station distribution. Figures 1b–1d show locations for 148 detected events from five different templates. Differential times are calculated separately for each template; common events among these templates allow the data to be combined and inverted simultaneously to estimate hypocenters for all events. Also notable is the small depth range for these events. Most locate within several hundred meters depth despite assumed initial depths randomized over a range of approximately 10 km.

[13] The lineation of tremor hypocenters in cross section (Figure 1d) is reminiscent of microearthquake "streaks", aligned in the direction of fault slip, which have been observed at shallower depths on primarily creeping faults [*Rubin et al.*, 1999; *Waldhauser et al.*, 1999, 2004]. As has been proposed for earthquake streaks, the tremor may concentrate at a geometric or frictional boundary. Further work is necessary to establish whether this "tremor streak" is a fixed feature or whether its depth or structure may vary over longer times. Interestingly, the depth of the located tremor is relatively close to the estimated Moho in this region [*Trehu and Wheeler*, 1987].

[14] The persistent correspondence between the strike of tremor locations and the strike of the SAF as well as the apparent alignment of tremor with the slip orientation suggest that these events occur on the deep extension of the fault, likely by a process of shear slip, similar to the mechanism argued for tremor in the Nankai trough subduction zone [*Shelly et al.*, 2006; *Ide et al.*, 2007; *Brown et al.*, 2008; *Ohta and Ide*, 2008]. At times we observe a clear migration of the tremor source along the fault to the NW or SE, at rates of 15–40 km/hr, as shown in Figure 2b. It is unclear whether the tremor migration velocity represents a rupture velocity, or if it is instead an apparent velocity as possibly ongoing deep deformation intersects the tremor-producing zone. The migration is similar to that observed in southwest Japan in the dip direction [*Shelly et al.*, 2007b], although the migration velocity of the Cholame tremor is slightly lower. Interestingly, the migrations in both settings appear to occur along the slip direction of the fault.

4. Location Uncertainty

[15] Absolute locations are constrained by P and S-wave arrival times for our master template LFE. Bootstrap analysis suggests 95% confidence interval of approximately ±3 km in depth and ±4 km horizontally (Figure S3). This range does not directly account for velocity model uncertainty; testing of several plausible velocity models suggests this could add up to 2 km of additional uncertainty. The tremors we locate lie slightly to the northwest and the depths are similar but much more concentrated compared to those located by *Nadeau and Dolenc* [2005].

[16] Relative locations will generally be much more precise than absolute locations, but will occasionally be subject to large errors. In particular, any cross-correlation cycle slips in our estimation of differential times will substantially affect the locations. We aim to prevent cycle slips by using stringent correlation thresholds and especially by calculating our differential times based on a cluster correlation sum, rather than a single station. While effective overall, this procedure sacrifices redundancy to gain accuracy. As we only obtain a single differential time for each cluster, we are left to estimate 4 parameters (3 spatial coordinates and time) for each event using only 4 data. While this provides no redundancy, events with one or more erroneous times can sometimes be eliminated when no consistent solution can be found. Assuming a dominant frequency of 4 Hz, a single cycle slip will result in a

differential time error of 0.25 seconds, a time during which an S wave in the deeper part of our model will propagate ~1 km. Primarily for this reason, we hesitate to interpret the scatter of events outside the main trend as a real feature. Imperfections in our velocity model will only minimally impact relative locations, since the distances between events are small.

5. Conclusions

[17] We examine Cholame tremor on October 6, 2007, locating a portion of this tremor with waveforms similar to an identified LFE template. The template is located in an absolute sense at ~26 km depth beneath the surface trace of the SAF. Similar events are located relative to this template, forming a near-linear structure striking parallel to the SAF, which likely represents the deep extension of the fault. This suggests that Cholame tremor is analogous to tremor observed in subduction zones and could be generated by shear slip beneath the main seismogenic portion of the fault. We also find a narrow range of depths for many events of several hundred meters or less. Tremor might be produced at a geometric or frictional boundary within the deep mostly-creeping zone of the fault. The alignment of tremor in a narrow zone near the base of the crust suggests that the SAF retains discrete structure through the entire crust and down to at least 10 km below the deepest regular earthquakes. Further work should be performed to determine whether the depth of the tremor varies over longer time periods. The current lack of any resolvable accompanying geodetic signal might be explained by the less episodic nature and smaller source region of tremor activity in this area [*Nadeau and Dolenc*, 2005], as compared with major episodes of tremor in the Cascadia or southwest Japan subduction zones. Although implications for seismic hazards remain to be determined, this portion of the fault merits close monitoring, as it may have been the nucleation point of the great 1857 Fort Tejon earthquake [*Sieh*, 1978].

[18] **Acknowledgments.** We thank the landowners who generously allowed instruments to be deployed on their property. Some of the seismometers were provided by the Geophysical Instrument Pool Potsdam (GIPP) of GFZ. A portion of this work was performed while D.R.S. was supported by the Miller Institute for Basic Research, University of California, Berkeley. Operational support for the HRSN provided through USGS grant 07HQAG0014. Research support provided through NSF grants EAR-0537641and EAR-0544730 and through USGS grant 06HQGR0167. We thank Cliff Thurber, Steve Malone, Justin Rubinstein and Jessica Murray-Moraleda for helpful and constructive reviews.

References

Brown, J. R., G. C. Beroza, and D. R. Shelly (2008), An autocorrelation method to detect low frequency earthquakes within tremor, *Geophys. Res. Lett.*, *35*, L16305, doi:10.1029/2008GL034560.

Cannata, A., M. Hellweg, R. M. Nadeau, and S. Gresta (2007), Detection method of low-frequency earthquakes in the non-volcanic tremor beneath the San Andreas Fault, *Eos Trans. AGU*, *88*(52), Fall Meet. Suppl., Abstract T21A-0356.

Gomberg, J., J. L. Rubinstein, Z. Peng, K. C. Creager, J. E. Vidale, and P. Bodin (2008), Widespread triggering of non-volcanic tremor in California, *Science*, *319*, 713.

Ide, S., D. R. Shelly, and G. C. Beroza (2007), Mechanism of deep low frequency earthquakes: Further evidence that deep non-volcanic tremor is generated by shear slip on the plate interface, *Geophys. Res. Lett.*, *34*, L03308, doi:10.1029/2006GL028890.

Johnston, M. J. S., R. D. Borcherdt, A. T. Linde, and M. T. Gladwin (2006), Continuous borehole strain and pore pressure in the near field of the 28 September 2004 M 6.0 Parkfield, California, earthquake: Implications for nucleation, fault response, earthquake prediction, and tremor, *Bull. Seismol. Soc. Am.*, *96*, doi:10.1785/0120050822.

Nadeau, R. M., and D. Dolenc (2005), Nonvolcanic tremors deep beneath the San Andreas Fault, *Science*, *307*, 389, doi:10.1126/science.1107142.

Obara, K. (2002), Nonvolcanic deep tremor associated with subduction in southwest Japan, *Science*, *296*, 1679–1681.

Obara, K., H. Hirose, F. Yamamizu, and K. Kasahara (2004), Episodic slow slip events accompanied by non-volcanic tremors in southwest Japan subduction zone, *Geophys. Res. Lett.*, *31*, L23602, doi:10.1029/2004GL020848.

Ohmi, S., I. Hirose, and J. J. Mori (2004), Deep low-frequency earthquakes near the downward extension of the seismogenic fault of the 2000 western Tottori earthquake, *Earth Planets Space*, *56*, 1185–1189.

Ohta, K., and S. Ide (2008), An accurate hypocenter determination method using network correlation coefficients and its application to deep low frequency earthquakes, *Earth Planets Space*, *60*, 877–882.

Rogers, G., and H. Dragert (2003), Episodic tremor and slip on the Cascadia subduction zone: The chatter of silent slip, *Science*, *300*, 1942–1943.

Rubin, A. M., D. Gillard, and J.-L. Got (1999), Streaks of microearthquakes along creeping faults, *Nature*, *400*, 635–641.

Shelly, D. R., G. C. Beroza, S. Ide, and S. Nakamula (2006), Low-frequency earthquakes in Shikoku, Japan and their relationship to episodic tremor and slip, *Nature*, *442*, 188–191.

Shelly, D. R., G. C. Beroza, and S. Ide (2007a), Non-volcanic tremor and low frequency earthquake swarms, *Nature*, *446*, 305–307.

Shelly, D. R., G. C. Beroza, and S. Ide (2007b), Complex evolution of transient slip derived from precise tremor locations in western S0hikoku, Japan, *Geochem. Geophys. Geosyst.*, *8*, Q10014, doi:10.1029/2007GC001640.

Sieh, K. E. (1978), Central California foreshocks of the great 1857 earthquake, *Bull. Seism. Soc. Am.*, *68*, 1731–1749.

Thurber, C., H. Zhang, F. Waldhauser, J. Hardebeck, A. Michael, and D. Eberhart-Phillips (2006), Three-dimensional compressional wavespeed model, earthquake relocations, and focal mechanisms for the Parkfield, California, region, *Bull. Seism. Soc. Am.*, *96*, S38–S49, doi:10.1785/0120050825.

Trehu, A. M., and W. H. Wheeler (1987), Possible evidence for subducted sedimentary materials beneath central California, *Geology*, *15*, 254–258.

Waldhauser, F., and W. L. Ellsworth (2000), A double-difference earthquake location algorithm: Method and application to the northern Hayward fault, *Bull. Seismol. Soc. Am.*, *90*, 1353–1368.

Waldhauser, F., W. L. Ellsworth, and A. Cole (1999), Slip-parallel seismic lineations on the northern Hayward Fault, California, *Geophys. Res. Lett.*, *26*, 3525–3528.

Waldhauser, F., W. L. Ellsworth, D. P. Schaff, and A. Cole (2004), Streaks, multiplets, and holes: High-resolution spatio-temporal behavior of Parkfield seismicity, *Geophys. Res. Lett.*, *31*, L18608, doi:10.1029/2004GL020649.

R. Bürgmann and R. M. Nadeau, Berkeley Seismological Laboratory, University of California, 211 McCone Hall, Berkeley, CA 94720, USA.

W. L. Ellsworth, G. S. Fuis, J. Murphy, and D. R. Shelly, U.S. Geological Survey, MS 977, 345 Middlefield Road, Menlo Park, CA 94025, USA. (dshelly@usgs.gov)

C. Haberland and T. Ryberg, GeoForschungsZentrum Potsdam, Telegrafenberg, D-14473 Potsdam, Germany.